Regulation of Non-Hermiticity in Spiral Microring Add-Drop Filters

Yihao Chen
School of Electronics and Information Engineering
Harbin Institute of Technology (Shenzhen)
Shenzhen, China
1172100333@stu.hit.edu.cn

Ke Xu
School of Electronics and Information Engineering
Harbin Institute of Technology (Shenzhen)
Shenzhen, China
kxu@hit.edu.cn

Xun Guan
Tsinghua-Berkeley Shenzhen Institute
Tsinghua Shenzhen International Graduate School, Tsinghua University
Shenzhen, China
xun.guan@sz.tsinghua.edu.cn

Yuanzheng Ma
Tsinghua-Berkeley Shenzhen Institute
Tsinghua Shenzhen International Graduate School, Tsinghua University
Shenzhen, China
myz22@mails.tsinghua.edu.cn

Jiawei Wang
School of Electronics and Information Engineering
Harbin Institute of Technology (Shenzhen)
Shenzhen, China
wangjw7@hit.edu.cn

***Abstract*—For on-chip optical cavities, various approaches have been investigated for steering the non-Hermiticity for realizing novel phenomena, such as exceptional points or PT-symmetry breaking. However, Here we report spiral microrings as an integrable deformed microcavity designed on silicon nitride-on-silica platform. By fine-adjusting the spacing between two spiral notches, the backscattering strength between clockwise and counterclockwise components can be controlled, which has been revealed in both simulation and experimental results.**

***Keywords*—non-Hermitian, spiral microring, backscattering**

I. Introduction

In nature, the vast majority of systems are open and can be described by a Hamiltonian. Such Hamiltonians exhibit special spectral degeneracies known as exceptional points (EP), at which two or more eigenvalues and the corresponding eigenvectors coalesce [1, 2]. For optical microcavities, the degeneracy of eigenvalues can serve as a basic element of a sensor because a small perturbation can lift the degeneracy and can therefore lead to a detectable splitting of these frequencies. [3]. In previous work, two nanosized scatterers have been commonly adopted to tune the non-Hermiticity of Hamiltonians [4]. In 2023, J. Li *et. al.* proposed and theoretically investigated non-Hermitian regulation in a spiral nanomembrane ring cavity [5], where the non-Hermiticity can be steered gradually to an EP without assistance of external scatterers. However, the concept of a spiral ring has not yet been verified experimentally on integrated photonic platform. Currently, we report control of non-Hermiticity using silicon

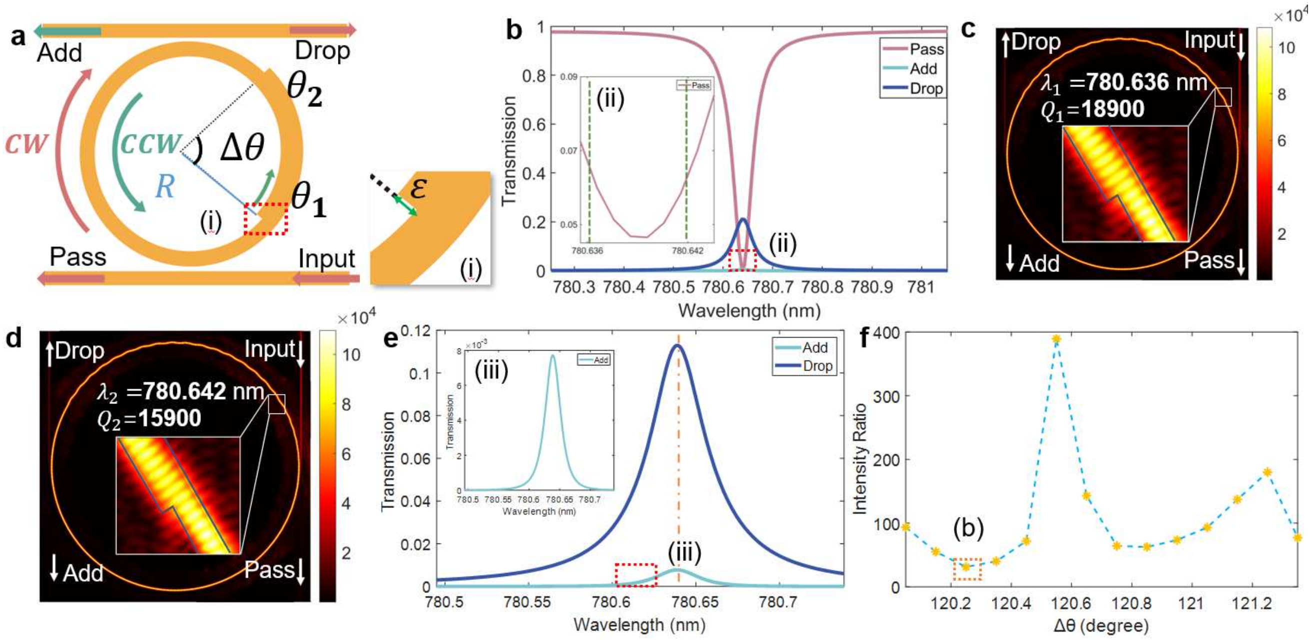

Fig. 1 | Device schematics and simulation results. (a) A spiral ring with an innermost radius of R, the spiral structure naturally forms two notches located at θ_1 and θ_2. (b) Simulated spectrum at the pass, drop, and add port, with $\Delta\theta$ = 120.25°. Inset: zoom-in view around the resonance. The dashed lines denote the eigenmodes with broken degeneracy. (c-d) Simulation electric field distribution with $\Delta\theta$ =120.25° at two eigenwavelengths of 780.636 nm (c) and 780.642 nm (d), respectively. (e) Zoom-in view of (b) showing the components at the add and drop ports. The orange line locate the wavelength point where to calculate the ratio of drop port to add port. (f) The calculated intensity ratio between drop and add ports as a function of $\Delta\theta$.

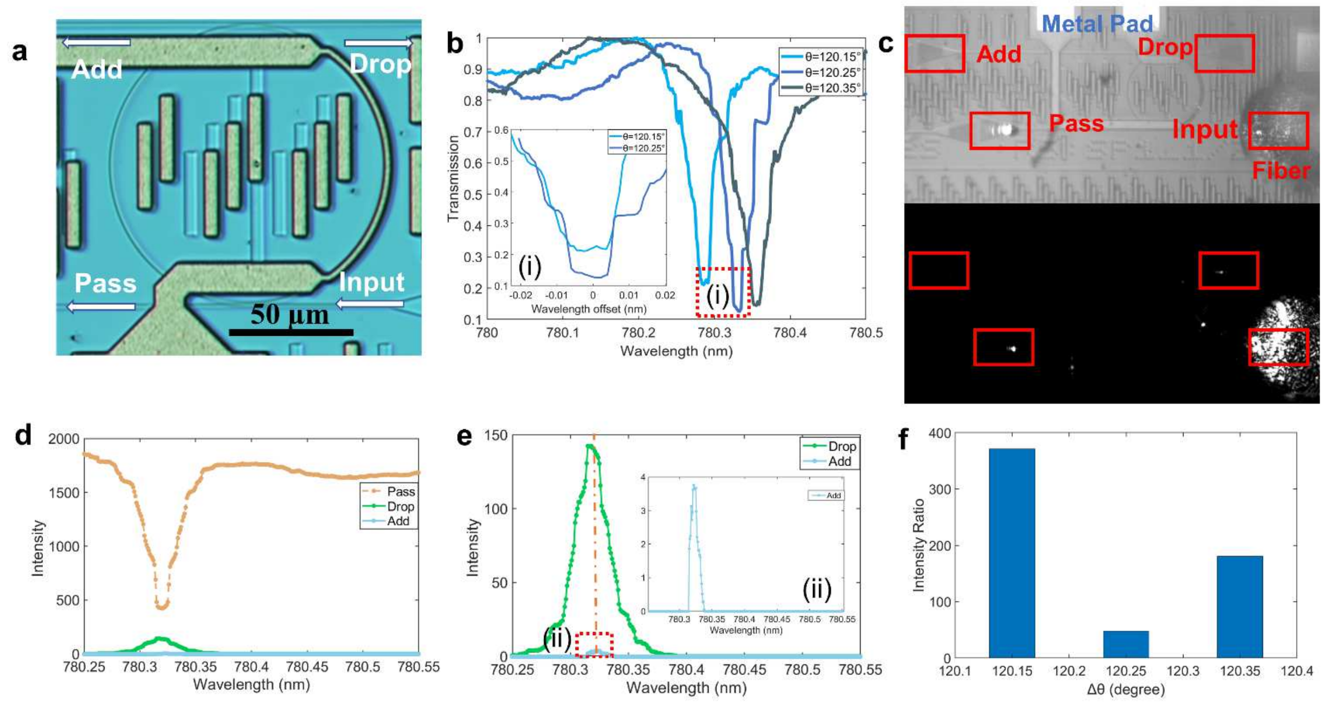

Fig. 2| Experimental demonstrations (a) microscope image of a SiN spiral ring resonator. (b) Measured spectra with $\Delta\theta$ = 120.15, 120.25 and 120.35°. Inset: comparison of resonances at $\Delta\theta$ =120.15 ° and 120.25°. (c) The device under test with whitelight illumination (up) and scattering signals (bottom). (d) Extracted spectrum based on collected signals at pass, drop, and add ports with $\Delta\theta$ = 120.25°. (e) Extracted spectrum based on collected signals at drop and add ports with $\Delta\theta$ = 120.25 °. (f) The calculated intensity ratio between drop and add ports as a function of $\Delta\theta$

nitride spiral microring add-drop filters. By adjusting the spacing of two notches of the spiral, we observed obvious changes in the weighting of clockwise (CW) and counterclockwise (CCW) components, and in experiment the ratio of lightwave components varied between ~370 and ~48.

II. PRINCIPLE

The effective Hamiltonian of the spiral microring system is given by a 2 × 2 non-Hermitian and non-symmetric matrix:

$$H = H_0 + H^{(N)} = \begin{pmatrix} E_0 & 0 \\ 0 & E_0 \end{pmatrix} + \begin{pmatrix} \Omega & \mathrm{A} \\ \mathrm{B} & \Omega \end{pmatrix} \qquad (1)$$

where the eigenvectors of the first matrix describe the equal CW(CCW) components in a circular cavity and the second matrix presents the effect of spiral notches. Ω is the complex mode shift introduced by the notches. The complex-valued off-diagonal elements A and B are the backscattering coupling coefficients. A (B) describes the backscattering from the CW (CCW) to the CCW (CW) components. Hence, we can regulate non-Hermiticity in the spiral ring by fine-adjusting the spacing between two spiral notches [5].

Here we design a structure in which the coupling strength of original non-degenerate modes can be fine-tailored by spiral notch-induced backscatterings [5]. As shown in Fig. 1a, the spiral ring structure in its top view follows the spiral function:

$$\rho(\theta) = R\left(1 + \frac{\varepsilon\theta}{2\pi R}\right) \qquad (2)$$

where R is the innermost radius, and θ is the azimuthal angle, and ε is the deformation parameter. The spiral ring structure does not terminate at the azimuthal angle of 2π but rather continues forward. In this way, we have created notches at the angle of θ_1 and θ_2 shown in Fig. 1a.

As two notches are located at different angular positions on the opposite side of a microring, the resulting strength of backscattering might be highly unbalanced, leading to an inherent chirality of eigenmodes[5].

III. RESULTS AND DISCUSSION

A. Simulation Results

We utilized COMSOL wave-optics module to carry out the simulations. The thickness of the waveguide layer was set to 0.15 μm, which matches the device thickness in our experiment. The radius R is 50 μm and we set the parameter ε to 0.25 μm. The parameter $\Delta\theta$ is fine-tuned. Fig. 1b shows simulated spectra at the pass, drop and add ports with the $\Delta\theta$ of 120.25. Due to the limited Q factor, the spectral offsets (~0.006 nm) between two eigenmodes cannot form clear splitting in the spectra. Nevertheless, two eigenstates can be calculated (see Fig. 1c-d).

The intensity of the drop port and add port directly reflect the level of backward scattering strength of notches, and also the weighting between the CW and CCW components. We employ the ratio of the intensity between the drop and add ports to evaluate the backscattering strength. When the ratio at the resonant wavelength (see orange line in Fig. 1e =) is higher (lower), it indicates a weaker (stronger) scattering strength. Fig. 1f displays the intensity ratio as a function of $\Delta\theta$, which was set from 120.05° to 121.35° with a step of 0.1° . The ratio indicates that the chirality of the probed mode is modulated.

B. Experiment Results

Our devices were designed with the IPKISS platform and manufactured by LIGENTEC. The 150nm-thick silicon nitride waveguide layer was fabricated with silicon oxide cladding. Fig. 2a shows the fabricated spiral microring structure. Fig. 2b shows measured spectra at the pass port around ~ 780 nm with a scanning step of 0.002nm. The resonant wavelength exhibits a redshift as $\Delta\theta$ increases, which is consistent with the trend in simulation results. This is attributed to a slightly prolonged effective optical lengths of the spiral ring upon an increased $\Delta\theta$.

As the scattering light at ~ 780 nm can be directly captured using low-cost CMOS camera, we recorded and analyzed the out-of-plane scattered light field distribution of the device. As shown in Fig. 2c, to get the intensity information of each port, we can perform intensity integration within the corresponding window at the grating coupler. Therefore, spectra can be extracted based on hyperspectral imaging at three ports, as shown in Fig. 2d. In this way, we can get the ratio of drop port to add port in the experiment more precisely rather than direct measurements using fiber coupling. Fig. 2f summarizes the dependence of the ratio on $\Delta\theta$ in the experiment. Similar to simulation results, the ratio exhibits obvious changes with the parameter $\Delta\theta$ and the maximum value is about 8 times the minimum value, which is close to the simulation data. It indicats that we have effectively regulated non-Hermiticity in the spiral ring by fine-tuning $\Delta\theta$.

IV. Conclusion

In this work, we have designed and fabricated spiral microrings that provides a potential integrable photonic platform for studying non-Hermitian properties. Both experimental and simulation results demonstrate the ability of regulating non-Hermitian properties by tuning the structural parameter $\Delta\theta$. In the following, the thermal modulation module can be leveraged to explore the richer possibilities of this structure.

Acknowledgment

This work is supported by the National Natural Science Foundation of China (Grant No. 62105080) and GuangDong Basic and Applied Basic Research Foundation (Grant No. 2023A1515011944).

References

[1] W. Chen, Ş. Kaya Özdemir, G. Zhao, J. Wiersig, and L. Yang, "Exceptional points enhance sensing in an optical microcavity," *Nature*, vol. 548, no. 7666, pp. 192–196, Aug. 2017, doi: 10.1038/nature23281.

[2] J. Wiersig, "Sensors operating at exceptional points: General theory," *PHYSICAL REVIEW A*, 2016, doi:10.1103/PhysRevA.93.033809

[3] J. Wiersig, "Enhancing the Sensitivity of Frequency and Energy Splitting Detection by Using Exceptional Points: Application to Microcavity Sensors for Single-Particle Detection," *Phys. Rev. Lett.*, vol. 112, no. 20, p. 203901, May 2014, doi: 10.1103/PhysRevLett.112.203901.

[4] H. Lee, T. Li, Z. Wang, A. Soman, A. Scallo, and T. Gu, "Spatially locked mode in defected microring resonators," 2019, doi： 10.1364/CLEO_QELS.2019.FTu4B.7

[5] J. li *et al.*, "Exceptional Points in a Spiral Ring Cavity for Enhanced Biosensing," *Journal of Lightwave Technology*, pp. 1–9, 2023, doi: 10.1109/JLT.2023.3237748.